ENHANCEMENT OF TENSILE PROPERTIES OF Al/SiC_p MMC SHEET BY OPTIMISATION OF SOLUTION TREATMENT

M.P. THOMAS, T. KILGOUR and J.E. KING

Department of Materials Science and Metallurgy, Pembroke Street, University of Cambridge, CB2 3QZ, U.K.

ABSTRACT

The microstructure, tensile properties and fracture behaviour of solution treated and naturally aged 2124 Al/SiC_p MMC sheet have been assessed as a function of solution temperature. Tensile properties follow approximate parabolic trends, initially increasing with solution temperature, reaching a peak and then decreasing as solution temperature continues to rise. Increasing the solution temperature dissolves more intermetallic particles. This reduces the area fraction of particles which appear on fracture surfaces and increases the tensile properties. At higher temperatures, surface oxidation, incipient melting and gas porosity cause the tensile properties to decrease. The optimum solution temperature is estimated to be 528°C. This is significantly above that commonly used for this family of MMCs.

KEYWORDS

Al/SiC_p MMC, tensile properties, solution treatment, intermetallic dissolution, gas porosity.

1. INTRODUCTION

One of the simplest ways to alter mechanical properties of a metal matrix composite (MMC) is to change the heat treatment. The majority of work in this area concentrates on the ageing behaviour of MMCs (Christman et al 1988; Davies et al 1990; Harris et al 1988; Hunt et al 1991; Lewandowski et al 1989; Wang et al 1990; You et al 1987). An area that has been neglected by researchers is that of solution treatment. Most MMCs are solution treated as though they were the unreinforced alloy. It has been shown that optimum properties of an MMC are to be found after significantly different ageing treatments than are given to the corresponding unreinforced alloy (Chrisman et al 1988; Harris et al 1988; Hunt et al 1991; Thomas et al 1993; Wang et al 1990). The optimum solution treatment for an MMC may also be significantly different to that commonly given to the unreinforced alloy.

2. MATERIAL

The material, supplied by B.P. Metal Composites Ltd., Farnborough, U.K., is a commercial 2124 Al-Cu-Mg alloy, reinforced with 20wt% (17.8vol%) of SiC particles (SiC_p) with a nominal size of 3μm - 5μm. The MMC was produced via a powder metallurgy route, extruded to plate and then rolled to 2mm thick sheet. The SiC_p is well distributed with little clustering and banding. The sheet had been annealed prior to this work.

3. EXPERIMENTAL PROCEDURE

"Dogbone" tensile specimens, with a 50mm gauge length and 17mm^2 nominal gauge cross section, were stamped out of the sheet with the tensile axis in the L (rolling) direction. Specimens were solution treated for two hours at temperatures between 485°C and 585°C, cold water quenched and naturally aged for at least 336 hours. All temperatures were controlled to ± 3°C. Tensile tests were conducted on a Schenk screw driven testing machine at a cross-head speed of 0.6mm/min. Elongation was monitored via a clip gauge mounted on the gauge length by means of knife edges. Load-elongation charts were recorded for each test, and from these the proportional limit (P.L.) i.e. limit of elastic behaviour, 0.2% proof stress (0.2% P.S.), ultimate tensile strength (U.T.S.), engineering strain to failure (e_f), work hardening exponent (n) and work hardening rate ($\Delta\sigma/\Delta\varepsilon$) were calculated. The work hardening exponent, n, was determined graphically using the equation:

$$\sigma = k\varepsilon^n \qquad (1)$$

using four points in the true strain range of $1x10^{-3} < \varepsilon < 4x10^{-3}$. $\Delta\sigma/\Delta\varepsilon$ was evaluated for the same strain interval. The Young's modulus (E) was estimated from the gradient of the elastic portion of load-elongation charts. The hardness of each specimen was measured using a Vickers macrohardness tester with a 10Kg load.

Each property was plotted against solution temperature. Polynomial curve fitting to each data set, followed by differentiation to find the point of inflexion, produced optimum solution temperatures for each property. The mean of these temperatures was taken as the overall optimum solution temperature for the MMC. Two specimens were solutioned at this optimum temperature and tested as above.

Polished sections of the MMC were examined by optical microscopy and image analysis, using a SeeScan Imager, to assess the variation in grain size and inclusion content with solution temperature. Fracture surfaces were studied both optically and in a Camscan S4 scanning electron microscope (SEM). Image analysis was conducted on photomicrographs of the fracture surfaces to assess the area fraction of fractured and/or de-bonded particles.

4. RESULTS

Tensile Properties The test results are given in Table 1 for each solution temperature.

TABLE 1: Effect of solution temperature on mechanical properties.

Solution Temp. °C	P.L. MPa	0.2% P.S. MPa	U.T.S MPa	e_f %	n	$\frac{\Delta\sigma}{\Delta\varepsilon}$ MPa	E GPa	Hardness Hv
485	265	382	561	5.3	0.091	17907	97	182.5
505	272	387	585	7.0	0.103	17098	99	200.2
525	296	403	621	9.7	0.086	16178	109	207.5
545	302	419	627	7.4	0.097	19071	116	215.9
565	276	403	566	5.4	0.101	19431	106	200.0
585	227	335	471	3.6	0.161	20775	88	180.5

All properties follow a parabolic-type curve as illustrated in fig.1 for the 0.2% P.S. and e_f. The overall optimum temperature is determined as 528°C.There is good agreement between properties for the optimum temperature, the standard deviation being $\sigma_n = 4.3$.

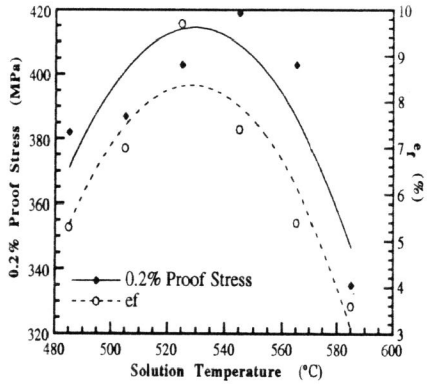

FIGURE 1: Polynomial curves fitted to 0.2% P.S. and e_f data.

The values of n and $\Delta\sigma/\Delta\varepsilon$ follow a reverse trend to the other properties, i.e. they show a minimum around 528°C rather than a maximum.

Table 2 compares the tensile properties of the sheet after solution treatment at a commonly used temperature and at the predicted optimum temperature of 528°C. Most work on 2XX4 series alloys uses a solution temperature between 495°C and 505°C (Davies et al, 1990; Harris et al, 1988; Kim et al 1992; Lin et al 1993; Logsdon et al 1986; Wang et al 1990; You et al 1987) so a temperature at the upper end of this range was chosen as "standard". The strengths, e_f, E and hardness are all increased by between 4% and 32% after the optimum solution treatment. The increase in e_f is accompanied by a decrease in n and $\Delta\sigma/\Delta\varepsilon$ of the MMC.

TABLE 2: Mechanical properties after standard (505°C) and optimum (528°C) solution treatments.

Mechanical Property	P.L. MPa	0.2% P.S. MPa	U.T.S MPa	e_f %	n	$\frac{\Delta\sigma}{\Delta\varepsilon}$ MPa	E GPa	Hardness Hv
Standard Specimen	272	370	585	7.0	0.103	17098	99	200.2
Optimum Specimen	336	394	622	8.6	0.077	16800	108	207.7

Microstructure Increasing oxidation of the MMC surface is seen (in the form of grey scale) as the solution temperature increases. At 585°C surface blistering is seen after quenching. These blisters are not seen if specimens are air cooled from this temperature. Optical examination of sectioned specimens shows blistering at 585°C and a high concentration of cavities in the surface layer at both 565°C and 585°C. These cavities are also seen, to a lesser extent, throughout the specimen cross section at temperatures above 545°C. There is a size dependence on cavity geometry, small cavities are rounded whilst larger ones are elongated in the L and T directions (fig.2).

Etching with Keller's Reagent reveals the grain structure; grains are equiaxed in the LT plane, but appear flattened in the ST and SL planes. Grain size appears to be limited by the SiC inter-particle spacing, with most grains extending between neighbouring SiC particles. Although no measurements of grain size have been made it is apparent that little or no grain growth occurs at any solution temperature.

Optical microscopy reveals a number of non-SiC inclusions in the MMC. Whitish, angular particles with sizes between 3μm - 7μm are clearly seen after light etching. Two types of inclusion are seen in the <3μm range. Black particles are visible before etching and more clearly after etching, whilst etching also reveals rounded, grey/white particles. Image analysis shows the area fraction of large, white particles and small grey/white particles to decrease with increasing solution temperature (fig.3).

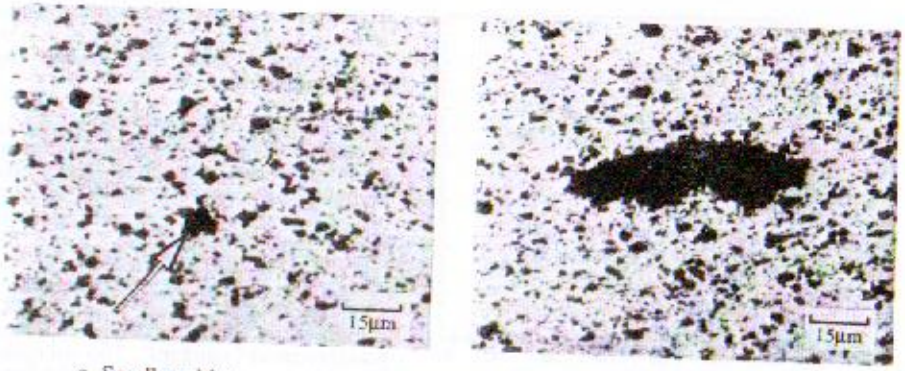

a. Small cavities

b. Large cavities

FIGURE 2: Size dependence of matrix cavity geometry.

SEM reveals similar fracture surfaces at all solution temperatures. The expected fracture mode, of void coalescence and growth, is seen in all specimens. The void size is bimodal: small matrix voids and larger voids associated with fractured particles. Very little particle debonding is seen. At 565°C and 585°C a few small areas of matrix have a faceted appearance. All specimens exhibit a small central section which failed perpendicular to the testing axis, surrounded by large shear regions containing elongated voids. The amount of shear is approximately the same at all solution temperatures. Image analysis of particles present on the fracture surfaces is shown in fig.4.

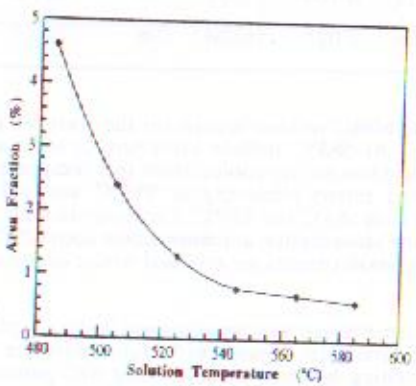

FIGURE 3: Area fraction of inclusions on polished sections of the MMC as a function of the solution temperature.

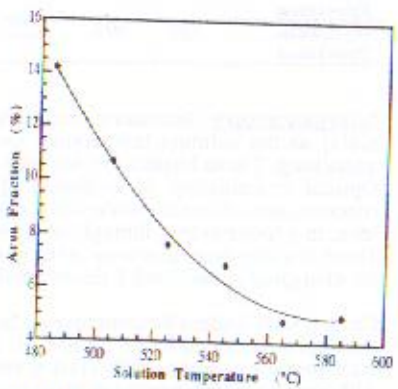

FIGURE 4: Area fraction of particles on MMC fracture surfaces as a function of the solution temperature.

The area fraction of particles decreases with increasing solution temperature. At temperatures above 545°C, matrix cavities become visible, their number increasing with increasing temperature. At 585°C surface blisters are seen, apparently formed from the coalescence of

smaller cavities, highly concentrated in the surface layer (fig.5).The interior of these blisters contain a "stalagmite/stalactite" structure (arrowed in fig.5b.)

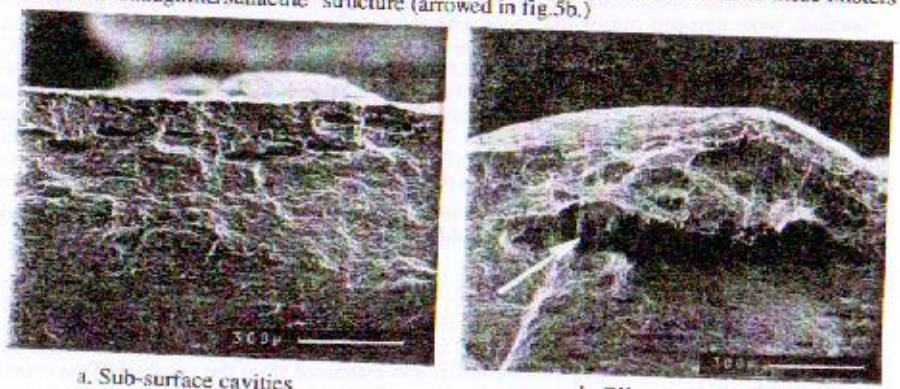

a. Sub-surface cavities

b. Blister

FIGURE 5: Blister formation from large near-surface cavities.

5. DISCUSSION

The parabolic nature of most property curves suggests that there is a competitive effect between property enhancement mechanisms at low solution temperatures and property degradation processes at high solution temperatures. The optimum solution temperature is very similar for each property, suggesting that the same mechanisms affect each property.

The inverse temperature dependence of n and $\Delta\sigma/\Delta\varepsilon$ compared to the other tensile properties is directly related to the change in ε_f. Generally speaking, when the work hardening of a material decreases, the ductility increases and vice versa. The change in work hardening behaviour of the MMC is not particularly large, as confirmed by the consistency of the fracture behaviour and fracture surface shear lip size.

The small, black particles seen in the matrix are oxide particles [Thomas et al 1993]. These are present due to the break-up, during MMC production, of the oxide film that coats the particles in the initial Al alloy powder. The temperature range used in this study will have no effect on these and they are not expected to play a part in the tensile property variation.

The whitish particles observed in this type of MMC have previously been identified as intermetallics [Ferry et al 1992] formed during the hot working of the MMC. The smaller particles tend to be coarse intermediate or equilibrium precipitates (in this case S and θ) whilst the larger ones contain Mn and impurity elements such as Fe and Si [Ferry et al 1992]. Increased solution temperature leads to increased dissolution of these particles. This has several beneficial effects. Intermetallic particles are known to be brittle and can fracture at low applied stresses [Ludtka et al 1982; Rios et al 1991] causing void formation and premature failure during tensile loading. Decreasing the intermetallic content reduces this effect. In addition, the elements contained in the intermetallic particles are returned to solution increasing solid solution strengthening and enhancing GPB zone formation during natural ageing.

Since brittle intermetallics fracture easily, fracture surfaces of the MMC are expected to contain disproportionately large numbers of these particles. Their dissolution as solution temperature increases corresponds to a reduction in the number of particles on the fracture surface, as the image analysis results in fig.4 show. Comparing the data in figs. 3 and 4 it is

apparent that the reduction in particle content on the fracture surface closely follows the reduction in intermetallic content in the matrix. The enhanced tensile properties of the MMC are, therefore, thought to be due to the dissolution of intermetallic particles. This process is essentially complete at 545°C, however, and the tensile properties are observed to decrease above 528°C. At higher temperatures, the positive effect of intermetallic dissolution must be outweighed by negative effects.

The increase in surface oxidation as solution temperature increases would be expected to decrease the properties of the MMC, since the surface layer is embrittled. This may be one mechanism for the reduction in properties at high solutioning temperatures.

At temperatures above the incipient melting point of the matrix alloy, local melting occurs in the low melting point constituents situated at grain boundaries. This embrittles the grain boundaries and leads to intergranular fracture and reduced tensile properties. In all specimens, however, evidence of incipient melting was minimal even at 585°C, which is well above the incipient melting point of the matrix alloy of 512°C (BP Metal Composites 1990). The areas of faceted matrix seen at 565°C and 585°C are attributed to intergranular fracture due to incipient melting. These areas were very small and infrequent indicating that incipient melting has a minor effect on fracture behaviour.

A more important phenomenon is the blistering and cavity formation. This is thought to be the main cause of the decrease in tensile properties at high temperatures. The elongated shape of large cavities follows the flattened grain structure of the matrix and suggests that they form at grain boundaries. The cavities appear to have been formed by gas pressure. Gas may come from a number of sources. The initial Al alloy powder is atomised under an Argon (Ar) shroud to minimise oxidation. During this process there is an amount of Ar pick-up which will not be completely eradicated by vacuum degassing. Some Hydrogen (H) may also be present if the atomising atmosphere contained moisture. Both gases are present in solid solution in the Al alloy powder and subsequent MMC at all processing temperatures. If the solution temperature is high enough, however, Ar and H mobility may be sufficient for them to migrate to, and cluster at, grain boundaries. With time cavities forms, nucleating spherically but elongating along grain boundaries as they grow (fig.2). The cavities become trapped in the matrix upon quenching causing porosity. Areas of incipient melting are particularly prone to gas porosity (Hunsicker 1984) due to the higher solubility of Ar and H in the liquid phase (Varley 1970). The Ar and H content of this MMC will not be very high and so only a low concentration of small cavities will form by this mechanism. They would also be expected to be evenly distributed throughout the MMC cross section. Whilst such porosity may be responsible for the even population of cavities in the central portion of the present MMC specimens, they cannot be responsible for the high concentration of large cavities near the surface, nor for the surface blisters.

The most likely cause of the surface cavities and blisters is H damage, caused by moisture either in the furnace or during quenching. This effect is commonly seen in unreinforced Al alloys solutioned in a moist furnace environment [Hunsicker 1984], leading to a decreasing population of cavities with increasing distance from the surface due to the limiting effect of H diffusion from the specimen surface. In the present case, this gradual decrease in cavity concentration is not seen. There is a surface layer of blisters and high cavity concentration and a much lower concentration of cavities throughout the rest of the cross-section. This, coupled with the fact that the blisters only appear upon quenching, suggests that the source of the H is the quench bath. When placed in the quench bath the MMC is sufficiently hot to form a blanket of steam around it. At the highest temperatures there is sufficient time for rapid diffusion of H into the surface layer. The high concentration of H causes gas cavities and blisters to form almost immediately. The temperature quickly drops, so that H diffusion beyond the surface layer is halted and the gas cavities become trapped in the MMC. Surface blisters appear to be formed from the very rapid coalescence of cavities (fig.5). This causes the small strands of matrix between neighbouring cavities to elongate and neck forming the "stalagmite/stalactite" structure seen in fig.5b.

The minimal grain growth with increasing solution temperature is expected to have a negligible effect on properties. Observations of the grain structure suggest that newly-recrystallised grains grew slowly during the original annealing process until they filled the SiC inter-particle spacing. At the range of temperatures used in this study, grain boundary pinning due to oxide, intermetallic and SiC particles prevents grain growth during the two hours of solution treatment. The grain pinning effect of particulate reinforcement has previously been noted in MMCs (Ferry et al 1993; Vyletel et al 1992).

6. CONCLUSIONS

1. Significant tensile property gains can be realised by increasing the solution temperature of this MMC from 505°C to 528°C.
2. Increasing the solution temperature leads to a decrease in the amount of inter-metallic in the matrix.
3. The reduction in intermetallic content is associated with a reduction in the number of particles appearing on the fracture surface.
4. High solution temperatures lead to problems of surface oxidation and gas porosity, via mechanisms involving H and/or Ar.
5. Negligible grain growth and only small amounts of incipient melting of the matrix occur, even at the highest solution temperatures.
6. The variation in tensile properties with solution temperature is a result of competition between the positive effects of intermetallic dissolution and improved solute strengthening/GPB zone precipitation versus the negative effects of surface oxidation, gas porosity and incipient melting.

ACKNOWLEDGEMENTS

The authors would like to thank Professor C.J.Humphreys for the provision of research facilities. One author (M.P.T.) acknowledges the financial support of the SERC and British Aerospace (Commercial Aircraft) PLC.

REFERENCES

BP Metal Composites 1990 "Material Safety Data Sheet BP217", BP Metal Composites, Farnborough

Christman T., Suresh S. 1988 "Effects of SiC Reinforcement and Aging Treatment on fatigue Crack Growth in an Al-SiC Composite", Materials Science and Engineering, Vol.102A, p.211

Davies C.H., Raghunathan N., Sheppard T. 1990 "The Structure/Property Relationship of SiC Reinforced RSP Aluminium Alloys. In: BNF 7th International Conference - The Materials Revolution Through the 90"s, Powders, Metal Matrix Composites, Magnetics. BNFL Metals Technology Centre, Oxon. Paper 30

Ferry M., Munroe P., Crosky A., Chandra T. 1992 "Microstructural Development During Cold Deformation and Recrystallisation of 2014 Al-Al_2O_3 Particulate Composite", Materials Science and Technology, Vol.8, p.43

Ferry M., Munroe P.R., Crosky A. 1993 "Grain Growth of an Aluminium 2014/Al_2O_3 PMMC During Solution Heat Treatment", Scripta Metallurgica et Materialia, Vol.28, p.1235

Harris S.J., Dinsdale K., Gao Y., Noble B. 1988 "Influence of heat treatment on the monotonic and fatigue properties of aluminium alloy composites". In: Mechanical and Physical Behaviour of Metallic and Ceramic Composites, 9th Risø International Symposium on Metallurgy and Materials Science. (Edited by: S.I.Anderson, H.Lilholt and O.B.Pederson). Risø National Laboratory, Denmark p.373

Hunsicker H.Y. 1984 "Metallurgy of Heat Treatment and General Principles of Precipitation Hardening". In: Aluminum - Properties and Physical Metallurgy (Edited by: J.E.Hatch). American Society for Metals, Ohio, p.152

Hunt E., Pitcher P.D., Gregson P.J. 1991 "Precipitation Behaviour in SiC Reinforced 8090 and 2124 MMC". In: Proceedings of the International Conference on Light Metals: Advanced Aluminium and Magnesium Alloys. (Edited by: T.Khan and G.Effenberg). American Society for Metals, Ohio, p.687

Kim Y.H., Lee S., Kim N.J. 1992 "Fracture Mechanisms of a 2124 Aluminium Matrix Composite Reinforced with SiC Whiskers", Metallurgical Transactions, Vol.23A, p.2589

Lewandowski J.J., Liu C., Hunt W.H. 1989 "Effects of Matrix Microstructure and Particle Distribution on Fracture of an Aluminum Metal Matrix Composite", Materials Science and Engineering, Vol.107A, p.241

Lin J.S., Li P.X. Wu R.J. 1993 "Aging Evaluation of Cast Particulate-Reinforced SiC/Al(2024) Composites", Scripta Metallurgica et Materialia, Vol.28, p.281

Logsdon W.A., Liaw P.K. 1986 "Tensile, Fracture Toughness and Fatigue Crack Growth Rate Properties of Silicon Carbide Whisker and Particulate Reinforced Aluminium Metal Matrix Composites", Engineering Fracture Mechanics, Vol.24, p.737

Ludtka G., Laughlin D.E. 1982 "The Influence of Microstructure and Strength on the Fracture Mode and Toughness of 7XXX Series Aluminum Alloys", Metallurgical Transactions, Vol.13A, p.411

Rios P.R., Bruno J.C., Fonseca A.S.M. 1991 "Influence of Coarse Inclusions on Strength, Ductility and Fracture of a Hot-Extruded AA2014 Aluminium Tube", Journal of Materials Science Letters, Vol.10, p.1346

Thomas M.P., King J.E. 1993 "The Effect of Thermal and Mechanical Processing on the Tensile Properties of Powder Formed 2124 Al and 2124 Al/SiC_p Metal Matrix Composite." Accepted for publication, Journal of Materials Science and Technology, Vols 9/10

Varley P.C. 1970 In: The Technology of Aluminium and its Alloys, Newnes-Butterworths, London, p.11

Vyletel G.M., Krajewski P.E., Van Aken D.C., Jones J.W., Allison J.E. 1992 "Effect of Cold Work on the Recrystallized Grain Size in a Particle-Reinforced Aluminum Alloy", Script Metallurgica et Materialia, Vol.27, p.549

Wang A., Rack H.J. 1990 "The Effect of Aging on the Abrasion Behaviour of SiC_w/2124 Metal Matrix Composite". In: Metal and Ceramic Composites: Processing, Modelling and Mechanical Properties (Edited by: R.B.Bhagat, A.H.Clauer, P.Kumar and A.M.Ritter). The Minerals, Metals and Materials Society, Pennsylvania, p.487

You C.P., Thompson A.W., Bernstein I.M. 1987 "Proposed Failure Mechanism in a Discontinuously Reinforced Aluminium Alloy", Scripta Metallurgica et Materialia, Vol.21, p.181